



Published in final edited form as:

Clin Cancer Res. 2014 August 15; 20(16): 4400–4412. doi:10.1158/1078-0432.CCR-13-1486.

PBX1 is a Favorable Prognostic Biomarker as it Modulates 13-*cis* Retinoic Acid-mediated Differentiation in Neuroblastoma

Nilay Shah^{1,#}, Jianjun Wang², Julia Selich-Anderson¹, Garrett Graham³, Hasan Siddiqui¹, Xin Li⁴, Javed Khan², and Jeffrey Toretsky³

¹Center for Childhood Cancer and Blood Diseases, The Research Institute of Nationwide Children's Hospital and The Ohio State University College of Medicine, 700 Children's Drive, Columbus, OH 43205

²Oncogenomics Section, Advanced Technology Center, Pediatric Oncology Branch, Center for Cancer Research, National Cancer Institute, National Institutes of Health, Gaithersburg, MD, 20877

³Department of Oncology, Georgetown University, Lombardi Comprehensive Cancer Center, 3970 Reservoir Rd NW, Washington, DC, 20007

⁴Department of Biostatistics, Bioinformatics and Biomathematics, Georgetown University, 3900 Reservoir Rd NW, Washington, DC, 20007

Abstract

Purpose—Neuroblastoma is an embryonic childhood cancer with high mortality. 13-*cis* retinoic acid (13-*cis*RA) improves survival for some patients, but many recur, suggesting clinical resistance. The mechanism of resistance, and the normal differentiation pathway, are poorly understood. **Three-Amino-acid Loop Extension (TALE)** family genes are master regulators of differentiation. Since retinoids promote differentiation in neuroblastoma, we evaluated TALE family gene expression in neuroblastoma.

Experimental Design—We evaluated expression of TALE family genes in RA-sensitive and -resistant neuroblastoma cell lines, with and without 13-*cis*-RA treatment, identifying genes whose expression correlate with retinoid sensitivity. We evaluated the roles of one gene, *PBX1*, in neuroblastoma cell lines, including proliferation and differentiation. We evaluated *PBX1* expression in primary human neuroblastoma samples by RT-qPCR, and three independent clinical cohort microarray datasets.

Results—We confirmed induction of *PBX1* expression, and no other TALE family genes, was associated with 13-*cis*RA responsiveness in NB cell lines. Exogenous *PBX1* expression in neuroblastoma cell lines, mimicking induced *PBX1* expression, significantly impaired proliferation and anchorage-independent growth, and promoted RA-dependent and -independent differentiation. Reduced *PBX1* protein levels produced an aggressive growth phenotype and RA resistance. *PBX1* expression correlated with histological neuroblastoma subtypes, with highest

[#]Contact Information for corresponding author: Nilay Shah, 700 Children's Drive, RBII WA4023, Columbus, OH, 43205. Phone number 614-722-2876, Fax number 614-722-5895. nilay.shah@nationwidechildrens.org.

None of the authors have any conflict of interest or financial disclosures related to this work.

expression in benign ganglioneuromas and lowest in high-risk neuroblastomas. High *PBX1* expression is prognostic of survival, including in multivariate analysis, in the three clinical cohorts.

Conclusions—*PBX1* is an essential regulator of differentiation in neuroblastoma and potentiates retinoid-induced differentiation. Neuroblastoma cells and tumors with low *PBX1* expression have an immature phenotype with poorer prognosis, independent of other risk factors.

Keywords

Neuroblastoma; Differentiation; 13-*cis* retinoic acid; *PBX1*

Introduction

Neuroblastoma (NB) is the most common extracranial pediatric solid tumor, representing 8% of childhood cancer diagnoses but 15% of childhood cancer-related deaths(1). The diverse clinical spectrum of NB presents numerous therapeutic challenges. Infant patients commonly present with low-grade disease, often with spontaneous regression, and some patients are managed expectantly with observation never requiring surgery(2). However, there are no validated biomarkers to predict which patients can be safely observed in contrast to those who would benefit from surgery and chemotherapy.

In contrast, >40% of patients present at diagnosis with aggressive disease and distant metastases(1). Patients with high-risk disease receive multi-agent chemotherapy, surgery, high-dose chemotherapy with autologous hematopoietic stem cell rescue(HDC-aHSCR), radiotherapy, immunotherapy with chimeric anti-GD2 antibody ch14.18, IL-2 and GM-CSF, and the differentiation agent 13-*cis* retinoic acid(13-*cis*RA). Despite intensive treatment and improved responses with the introduction of immunotherapy(3), up to 40% of high-risk patient tumors progress during induction chemotherapy(4) and 5-year disease-free survival remains <50%(5). Identification of *MYCN* amplification as a prognostic biomarker of aggressive disease radically improved risk stratification and treatment of NB(6). Since the seminal discovery of *MYCN*, additional clinical and genetic biomarkers have been identified, but connection of these factors to NB biology or tumor aggression remains cryptic, particularly in tumors without *MYCN* amplification(7, 8).

NB is a prototypic embryonic cancer with demonstrated aberrations in normal developmental pathways(9, 10). The HOX genes are master regulators of development in animals; select HOX gene expression, including *HOXC6* and *HOXC9*, has been associated with NB differentiation, response to 13-*cis*RA, and outcome(11, 12). HOX proteins critically interact with cofactors, including members of the **Three-Amino-Acid Loop Extension(TALE)** gene family. The TALE family genes (*PBX1-4*, *MEIS1-3*, and *PKNOX1-2*), like HOX genes, are critical to tissue differentiation(13), including retinoid-induced differentiation(14). Expression of *PBX1-3* is regulated by retinoids in other cell types(15) and has been shown to direct endogenous retinoid synthesis within the nervous system(16). A comprehensive study of the expression of all TALE gene family members has not been previously performed in NB.

The functions of TALE family genes are temporospatially specific, with the same gene often having divergent functions in different tissues. For example, *PBX1* is necessary for normal pancreatic development(17) and behaves as a tumor suppressor in prostate cancer(18). In contrast, *PBX1* is implicated as an oncogene in breast cancer(19) and melanoma(20), and *PBX1* is oncogenic in leukemia as part of the E2A-PBX1 fusion protein(21). The functional complexity is increased by gene paralogs (e.g. *PBX1-4*), which can have distinct or overlapping functions within a given tissue. These varying but important roles make it critical to evaluate these genes specifically in neuroblastoma to define their roles in oncogenesis.

Here, we perform the first comprehensive analysis of TALE family gene expression in NB. We demonstrate that, among TALE family genes, only *PBX1* expression is associated with responsiveness to 13-*cis*RA in NB. We confirm *PBX1* induces neuronal differentiation and increases sensitivity to 13-*cis*RA. Furthermore, we show *PBX1* expression is directly associated with decreased proliferation independently of 13-*cis*RA. Finally, we demonstrate *PBX1* expression in primary human tumors is associated with low tumor grade and patient survival. *PBX1* expression may thus serve as a biomarker in low-risk disease by identifying patients who may be observed without intervention. In high-risk disease, *PBX1* may stratify those patients for whom current therapies are ineffective, directing them to novel therapies.

Materials and Methods

Cell lines

Cell lines SK-N-SH, LAN-5, IMR-32, SK-N-BE(2), and SK-N-RA were obtained from Javed Khan; SMS-KAN and SMS-KANR from Joanna Kitlinska (via Children's Oncology Group(COG) MTA with Georgetown University); NBL-WS and LAI-5S from Susan Cohn (University of Chicago); SHSY5Y from ATCC; CHLA-15, CHLA-42, CHLA-90, CHLA-136, and LAN-6 from COG Cell Culture Repository; and HEK293T from OpenBioSystems. All were previously characterized (22–28). A table of the MYCN status of each cell line is in the Supplementary methods. CHLA-15, CHLA-42, CHLA-136, and CHLA-90 were grown in IMDM with 20% FBS (Hyclone) and 0.1% ITS (Corning). All other cell lines were grown in RPMI with 10% FBS. All parental and modulated cell lines were tested and authenticated by PowerPlex16 STR analysis (Promega) by the Nucleic Acids Core laboratory at Nationwide Children's Hospital(NCH), last in December 2013 and January 2014. To note: the SK-N-RA cell line was initially labeled as SK-N-AS when received but has been characterized by STR analysis to be the SK-N-RA cell line, including aliquots of the original cell line received from the Khan lab, all generated modulated cell lines, and the aliquots of the cell lines at the end of the studies. Dr. Khan's lab has confirmed the cell line they are using labeled SK-N-AS is, by STR, truly SK-N-AS, so we can only surmise our cell line was mislabeled, but it has been characterized to be consistent with SK-N-RA as published elsewhere. Although we performed the studies under the supposition that the cells were of SK-N-AS origin, the cells were always of SK-N-RA origin, and the presented data have been interpreted accordingly.

Plasmid construction and transfection

PBX1 cDNA plasmid(MHS1768-101376233), *PBX1*-shRNA set(RHS4531-EG5087), and nonsilencing negative control were purchased from OpenBioSystems. *PBX1* cDNA was cloned into pCDNA3.1+/Hygro(LifeTechnologies) or pLPCX(Clontech) and transfected using Lipofectamine2000(LifeTechnologies). shRNA plasmids were transfected into HEK293T cells with pHR-8.2 R and pVSVG packaging vectors. Generated viral supernatant was applied to NB cells. Cells were selected with hygromycin(200 µg/mL) or puromycin(1–7 µg/mL) for two weeks, then retreated monthly.

Human tumor and RNA samples

Primary ganglioneuromas(n=7) and neuroblastomas(low-risk, n=11, intermediate-risk, n=5) were obtained from Johns Hopkins University(JHU) pathology archives under IRB exemption and waiver of consent. Patient and sample characteristics, and tissue and data management are fully described in Supplemental Methods. RNA from high-risk neuroblastoma (INSS criteria, n=40) were obtained from the COG Neuroblastoma Tumor Bank, 20 from patients alive without disease progression, and 20 from patients dead of disease. Patient and treatment characteristics are described in Supplementary Methods. COG samples were obtained after informed consent and IRB approval. PHI was sequestered by COG and JHU, and IRB exemption granted by Georgetown University and NCH.

13-*cis*RA treatment and morphology studies

24 hours after seeding in complete media, cell lines were cultured in media with 10µM 13-*cis*RA (Sigma-Aldrich) or 0.1% DMSO. At 50–75% confluence, 100 cells were counted, in triplicate, and assessed for neurite extension, defined as neurite length – soma length(29). For RNA and protein analysis, cells were cultured for 7 days then collected in PBS; RNA was extracted as above, and protein extracted with RIPA buffer.

WST-1 Proliferation and 13-*cis*RA-survival analysis

5000 cells/well were plated in 96 well-plates in complete media, in triplicate, on 5 plates each. After 24 hours, one plate was treated with WST-1, 10%v/v(Roche) for 1 hour, then absorbance at 450nm (670nm reference) measured, and each triplicate was averaged. These values were used to normalize cell count and set as time 0. Media was changed on the remaining plates to complete media with 0.1% DMSO or 10µM 13-*cis*RA. Every 48 hours, one plate was treated with WST-1 and absorbance measured as above, then normalized for each derived cell line to time 0 values to calculate percent viability. Normalized absorbances were compared to control cells for each cell line set. Experiments were performed three times.

RT-qPCR

2 µg (cell lines) or 200 ng (primary tumors) of RNA were used in cDNA synthesis by Superscript VILO (LifeTechnologies), per manufacturer protocol. Yields were diluted per protocol and 2 µL of resulting product used in qPCR, using the Eppendorf RealPlex Mastercycler and KiCqStart Mastermix (Sigma Aldrich), per manufacturer protocols. qPCR was performed for 40 cycles, and T_m analysis used to confirm purity of PCR amplification.

Primers are listed in Supplementary Methods. Relative gene expression was calculated using the C_t method, using *18SRNA* as reference, and samples compared to SHSY5Y cells grown in complete media for normalization. Samples were tested in triplicate on three separate experiments.

Western Blots

Western Blots were performed with 50 μ g of cell lysate from each sample electrophoresed through 4–12% Bis-Tris Bolt™ gels (Life Technologies), then transferred onto PVDF membranes. Antibodies and full protocols are listed in Supplementary Methods.

Immunofluorescence

Cells were grown in complete media with DMSO or 10 μ M 13-*cis*RA for 5 days, then passaged onto CultureSlides (BD Biosciences) and grown for another 2 days. TUBB3 was evaluated by immunofluorescence, per manufacturer protocol (Cell Signaling). Cells were counterstained with Prolong AntiFade Mounting Media with DAPI (Life Technologies), and imaged under 40X magnification.

Soft Agar Colony Formation Assay

5000 cells/well were suspended in 0.3% LMP Agarose/RPMI Media+10% FBS in 6-well plates. Cells were plated in triplicate and cultured for 4 weeks, then stained with MTT solution. Wells were photographed and colonies counted.

Statistical Analysis, including Survival Analysis

Experiments were analyzed using GraphPad Prism6 software, except survival analyses of the expression datasets (30–32), described below. Data were tested by Student's t-test, one-way ANOVA, or two-way ANOVA as indicated.

Characteristics of the three published datasets have been previously described fully, including sample inclusion, clinical characteristics, and analysis methods (30–32). Survival data for Khan and Seeger datasets were obtained from the Oncogenomics website, annotated by the Oncogenomics section, Pediatric Oncology Branch of the National Cancer Institute. Survival data for the Oberthuer dataset were obtained from the Journal of Clinical Oncology, directly annotated by the primary researchers, including patient and outcomes data. The primary objective of survival studies was to investigate *PBX1*-expression association with survival, in the presence of other factors. EFS and OS were examined. Data was right-censored per patient status. INSS stage was grouped into elementary (stage 1, 2, and 4S) or advanced (Stage 3 and 4). Kaplan-Meier plots were generated to compare EFS and OS based on *PBX1* expression, classified into “high” and “low” groups. According to *a priori* knowledge and univariate analysis, five factors - *PBX1* expression, histology, age at diagnosis, INSS stage and *MYCN* amplification - were chosen for regression analysis with Cox-proportional-hazards model. Statistics were calculated by R Statistical Analysis package.

Results

Induction of *PBX1* is associated with retinoid sensitivity in NB cell lines

We evaluated *PBX1* expression in NB cell lines in response to 13-*cis*RA, utilizing 6 RA-sensitive and 4 RA-resistant cell lines. RA resistance was defined as no morphologic differentiation or apoptosis after treatment with 10 μ M 13-*cis*RA (Supplementary Figure 1A). Basal *PBX1* expression was variable across cell lines (Figure 1 and 2), with lowest expression in RA-resistant CHLA-15 cells. Notably, after treatment with 13-*cis*RA, RA-sensitive cell lines all had significant increases in *PBX1* expression, from 2.2-fold to 6-fold increase (Figure 1B), whereas RA-resistant cell lines had no significant increase in *PBX1* expression ($p=0.014$). We evaluated the expression of other TALE family genes, and none were consistently altered in association with RA sensitivity (Supplementary Figure 1B). These findings suggested *PBX1* is unique among TALE family genes in response to 13-*cis*RA in NB.

The *PBX1* mRNA changes were corroborated by protein expression. We treated 14 NB cell lines (4 RA-resistant, 10 RA-sensitive) with either 13-*cis*RA or DMSO for 5 days, then performed western blots for PBX1. We also evaluated MYC and MYCN expression, which are downregulated in RA-sensitive cells by 13-*cis*RA(33, 34), and NTRK1 and NTRK2, which are upregulated in response to 13-*cis*RA(35). Expression of these proteins in primary tumors correlates with clinical outcomes(36, 37). We confirmed the increase of PBX1 expression, observed as isoforms PBX1a and PBX1b, in RA-sensitive cell lines treated with 13-*cis*RA, and associated with changes in MYCN, MYC, NTRK1, and/or NTRK2 (Figure 2A–C). PBX1 expression did not increase in RA-resistant cell lines (Figure 2D).

PBX1 directly induces differentiation in NB cell lines

We studied the effects of *PBX1* in NB and RA-mediated differentiation using four cell lines: RA-resistant, MYCN-nonamplified SK-N-RA cells, the RA-sensitive, MYCN-nonamplified cell lines SK-N-SH and SHSY5Y (previously derived as an N-type subclone of the parental SK-N-SH), and the RA-sensitive, MYCN-amplified SK-N-BE(2) cells. We specifically used these cell lines to model induction of PBX1 expression, mimicked by exogenous expression, or blockade of that induction by use of shRNAs, using empty vector-transfected or nonsilencing shRNA-infected cells as controls. We measured *PBX1* mRNA levels in the generated cell lines by RT-qPCR, then confirmed protein expression changes by western blot (Figure 3). We reduced PBX1 expression to <20% of control in all cell lines (Figure 3, shPBX1 #3–#5). We increased PBX1 expression in SK-N-RA cells to 10–35 fold of control (Figure 3D), but only 3–8 fold of control in the RA-sensitive cell lines, as measured by RT-qPCR (Figure 3A–C), comparable to levels observed in parental cell lines treated with 13-*cis*RA (Figure 1A)

We used the stably-derived NB cell lines to assess the effects of the induction or blockade of PBX1 expression upon NB differentiation (Figure 3). The expression of the neuronal differentiation marker TUBB3 (29) and of retinoid-induced differentiation markers MYCN, MYC, NTRK1, and NTRK2 were evaluated in the cells grown in complete media with 13-*cis*RA or vehicle. In all cell line sets, without 13-*cis*RA, PBX1 expression correlated with

increased expression of either NTRK1 or NTRK2 compared to controls, and decreased expression of MYCN or MYC (Figure 3 immunoblots), and correlated with increased expression of TUBB3 in the SHSY5Y and SK-N-RA sets. When treated with 13-*cis*RA, these expression changes were amplified in RA-sensitive cells with increased PBX1 expression (Figure 3A–C). SK-N-RA cells with exogenous PBX1 expression also had increased protein levels of TUBB3 and NTRK2, but not NTRK1, compared to treated control cells (Figure 3D, PBX1 lanes). In all cell lines reduction of PBX1 expression reduced NTRK1 and NTRK2 expression, and, to a lesser extent, TUBB3 expression. Furthermore, blockade of RA-induced increase in PBX1 expression by shRNA prevented increased expression of these proteins when treated with 13-*cis*RA.

NB differentiation is also characterized by morphologic changes including neurite extension and/or cell lengthening(29). Microscopy demonstrated increased PBX1 expression was associated with increased neurite extension and cell lengthening, similar to control cells treated with 13-*cis*RA. In the SK-N-SH vector-control cells, <20% cells grow neurite extensions in complete media with vehicle (Figure 4). Neurite outgrowth is seen after 7 days of treatment with 10 μ M 13-*cis*RA in 76% of control cells. In SK-N-SH cells with 2–3-fold increased PBX1 levels, neurite extensions spontaneously develop in 53% of cells without 13-*cis*RA, and 90% of cells with 13-*cis*RA. Strikingly, clonal populations with higher PBX1 expression (>5x control cells) formed spindle-shaped cells with long neurites (Figure 4A, row 3) and virtually no proliferation (Figure 5), without exogenous 13-*cis*RA. However, they remain fully viable in culture for >8 months, able to readhere after trypsinization and extend neurites without any appreciable mitosis. This phenotype is consistent with a state of terminal differentiation. <10% of cells with repressed PBX1 expression, in contrast, grew neurite extensions even when treated with 13-*cis*RA (Figure 4A, rows 4 and 5). Similar results were observed in SHSY5Y cells and SK-N-BE(2) cells (Figure 4B, Supplementary Figure 2A–B).

TUBB3 is a neuron-specific cytoskeletal component(38). In differentiating neuroblasts, it relocates from a generalized cytoplasmic distribution to within elongating neurites. In the three cell lines tested, immunofluorescence for TUBB3 showed a direct association of expression and relocalization with increased PBX1 expression. In SK-N-SH and SHSY5Y cells, exogenous PBX1 expression caused relocalization of TUBB3 along neurites in the absence of 13-*cis*RA, similar to control cells treated with 13-*cis*RA (Figure 4C, Supplementary Figure 2C–D). Cells with repressed PBX1 expression had decreased or absent TUBB3 expression and no relocalization. Though SK-N-RA cells did not show significant morphologic changes with PBX1 expression changes, cells with increased PBX1 levels also had increased TUBB3 expression by immunofluorescence (Supplementary Figure 2E).

PBX1 expression suppresses neuroblastoma cell proliferation and sensitizes cells to the effects of 13-*cis*RA

We assessed the effects of PBX1 on NB cell proliferation in monolayer culture. Amongst the four cell lines, cells with increased PBX1 expression proliferated significantly more slowly than vector control over 96–192 hours (Figure 5; $p < 0.01$ or less for each cell line). In

SK-N-SH cells, clonal populations with >5-fold increase in PBX1 expression demonstrated virtually no proliferation (Figure 5A, PBX1 Clone 1, $p < 0.001$ versus vector control). Cells with decreased PBX1 expression proliferated significantly faster than control ($p < 0.05$ for each cell line). We noted that *rates* of proliferation were stable or increased over time in cell lines with reduced PBX1 expression, despite increasing confluency, and decreased with time in cell lines with increased PBX1 expression despite subconfluency (Supplementary Figure 3).

We originally observed that increased PBX1 expression in NB cell lines correlated with RA sensitivity (Figure 1 and 2). Accordingly, we hypothesized PBX1 expression was not only induced by 13-*cis*RA but also critical to responsiveness of the cells to RA. Indeed, we found that repression of PBX1 expression induced resistance to 13-*cis*RA, with increased proliferation compared to vector control (Figure 5A, $p < 0.01$ for all cell lines). Increased PBX1 protein levels significantly increased RA-sensitivity in all cell lines. That effect was greater and dose-dependent in natively RA-sensitive cell lines (SK-N-RA, $p < 0.05$; SK-N-SH, $p < 0.05$ – 0.001 ; SHSY5Y and SK-N-BE(2) $p < 0.001$). The SK-N-SH and SHSY5Y PBX1 clonal populations with highest PBX1 expression showed no significant proliferation after 8 days of 13-*cis*RA treatment ($p < 0.001$). These results show that PBX1 affects differentiation directly and also mediates the effects of RA upon NB cells.

We studied the effects of PBX1 expression on anchorage-independent growth in soft agar. In the three cell lines tested, increased PBX1 expression caused significant suppression of colony formation, and reduced PBX1 expression increased colony number (Figure 5B–C; $p < 0.001$ for SK-N-RA cells, $p < 0.0001$ for SK-N-SH and SHSY5Y cells, vs vector controls). Increased PBX expression caused near-total suppression of colony formation in SK-N-SH cells (Figure 5B, 2nd row, 2nd column), again consistent with terminal differentiation.

PBX1 expression correlates with neuroblastoma pretreatment risk classification and patient outcome

Current NB pretreatment risk stratification follows the guidelines established in the International Neuroblastoma Staging System (INSS)(39) or the International Neuroblastoma Risk Group (INRG) Classification system(5). Both systems use anatomic, histologic, and molecular criteria to establish at diagnosis patient risk from disease, which is used to guide the treatment approach for each patient. We evaluated the correlation of *PBX1* expression with current pretreatment risk classification and patient outcomes in primary human tumors and in three independent cohorts of human tumor data.

RNA was obtained from pretreatment primary tumors, including benign ganglioneuromas (GN, $n=7$), low-risk NB without recurrence after surgery (LR-NB, $n=8$), low-risk NB treated with chemotherapy after recurrence (LRR, $n=3$), intermediate-risk NB cured with surgery and chemotherapy (IR-NB, $n=5$), and high-risk NB (HR-NB, $n=40$). *PBX1* expression, measured by RT-qPCR, was normalized to untreated SHSY5Y cells as a baseline (Figure 6A, Supplementary Table 1). In these samples, *PBX1* expression was associated significantly with risk group and outcome. Expression was highest in GN; most had 2 log-fold higher expression than SHSY5Y cells. LR-NB samples had significantly lower expression than GN samples ($p < 0.001$), but 1-log fold higher than samples from patients who

needed chemotherapy for definitive cure (LR-NB vs. IR-NB or LRR; $p < 0.001$). HR-NB samples had significantly lower expression than the GN or LR-NB groups ($p < 0.001$), but subset analyses showed no significant difference between survivors and nonsurvivors in MYCN-amplified HR-NB (Supplementary Figure 4A, $p = 0.12$) or MYCN-nonamplified HR-NB ($p = 0.22$).

We next evaluated *PBX1* as a prognostic marker in NB in three independent gene expression datasets of clinical NB samples, with matching outcome data. The first dataset (hereafter referred to as the “Oberthuer” dataset) included data from 251 primary tumors from patients across the clinical spectrum, including all stages and MYCN amplification status, treated on German Neuroblastoma clinical trials NB90-NB2004(30). High *PBX1* expression was significantly prognostic of overall survival (OS) and event-free survival (EFS) in univariate analyses (Figure 6B: OS, $p = 0.0004$; Supplementary Figure 4B, EFS, $p = 0.00016$). Data on INSS criteria were available for the Oberthuer dataset. Multivariate analysis comparing *PBX1* expression with INSS risk factors confirmed that high *PBX1* expression is independently a favorable prognostic marker in these patients (EFS hazard ratio (HR) 0.49, 95% CI 0.28–0.87, $p = 0.0144$; OS HR 0.55, 95% CI 0.31–0.96, $p = 0.03653$, Supplementary Table 2), and a stronger biomarker than most factors currently used in INRG risk classification.

The second dataset (the “Khan” dataset) consisted of primary tumors from patients presenting with low- and high-risk disease, including tumors with either MYCN amplification or nonamplification(31). The dataset included 30 patients < 18 months of age and 19 patients > 18 months of age; 12 samples were also included in the Oberthuer dataset (3 low-risk, 4 intermediate-risk 6 high-risk, per INSS). All patients received treatment similar to current approaches, including 13-*cisRA* but not immunotherapy, based on risk classification. In these patients, high *PBX1* expression was prognostic of overall survival in univariate analysis (Figure 6C, $p = 0.00125$). INSS classification data, including age at diagnosis, stage, and MYCN amplification, was available for these patients. In multivariate analysis, *PBX1* was a favorable prognostic marker for OS that trended toward statistical significance (OS HR 0.4639, 95% CI 0.15–1.43, $p = 0.18$, Supplementary Table 3). Amongst patients < 18 months of age, the three patients who died of disease had significantly lower *PBX1* expression than the 27 patients who survived (Supplementary Figure 4C, $p = 0.005$). Patients with high-risk, MYCN-nonamplified disease represent a group for which there are no validated biomarkers predictive of response to treatment. Amongst these patients in the Khan cohort, survivors had significantly higher *PBX1* expression than nonsurvivors (Supplementary Figure 4D, $p = 0.0145$).

The third dataset used for survival analysis (the “Seeger” dataset(32)) consisted of 102 patients with metastatic, MYCN-nonamplified disease at diagnosis. These patients (intermediate risk, $n = 28$; high-risk, $n = 74$) were treated with multiagent chemotherapy, including a subset of patients who also HDC-aHSCR with or without 13-*cisRA* ($n = 23$). High *PBX1* expression strongly correlated with overall survival in univariate analysis (Figure 6D, $p = 0.0002$); annotated patient data was not available for multivariate analysis.

We evaluated if other TALE family gene expression correlated with clinical course. No other TALE gene significantly stratified outcome in all three databases in univariate analysis (Supplementary Table 4).

Discussion

Neuroblastoma is a cancer with inherently aberrant differentiation(9, 40). This is the first comprehensive evaluation in NB of the TALE gene family, known regulators of differentiation. In low-risk NB there are no validated biomarkers that identify patients who can be safely observed without surgery nor those who require chemotherapy to prevent recurrence Two challenges in high-risk patient management 1) identification of patients with RA-resistant disease and therapeutic alternatives 2) identification and therapeutic targeting of mechanisms of disease aggression in *MYCN*-nonamplified disease. Our experimental findings combined with the key findings from three clinical datasets identify *PBX1* as a potential physiologic node in both low-risk NB and high-risk *MYCN*-nonamplified disease. As a network node, *PBX1* would serve as a novel prognostic biomarker and therapeutic target.

Prior investigations into RA signaling in NB have identified few clinically relevant biomarkers of RA resistance, including *HOXC9*(12) and the *NFI/ZNF423* axis(41). In contrast to those studies, our conclusions are supported by experiments in multiple human NB cell lines and in multivariate analysis of three independent clinical datasets, supporting the role of *PBX1* as a biomarker of disease severity across clinical presentations of NB. More importantly, we show that *PBX1* expression not only is induced by 13-*cisRA* *in vitro*, but also potentiates its effects, suggesting that therapeutic approaches to increase its expression in neuroblastoma would improve the efficacy of 13-*cisRA*.

We demonstrated that *PBX1* is a critical component in NB differentiation, unique amongst TALE family genes. In cell lines treated with 13-*cisRA*, *PBX1* mRNA and protein expression was induced only in those cell lines sensitive to the effects of the drug, as demonstrated by associated morphologic and expression changes (Figures 1 and 2). We did appreciate a discordance between mRNA and protein expression within a given cell line (e.g., SK-N-RA) suggesting additional posttranscriptional regulation of expression. Nonetheless, the pattern of induction of *PBX1* expression was consistent between mRNA and protein, supporting a transcriptional induction in response to 13-*cisRA*

We modeled the effects of RA-mediated induction of *PBX1* by modulating its expression in NB cell lines. Our data showed *PBX1* expression correlated with cell growth and differentiation in RA-sensitive and resistant cell lines. Specifically, reduced *PBX1* expression increased proliferation and abrogated responsiveness to 13-*cisRA* in three RA-sensitive cell lines. Exogenous *PBX1* expression, mimicking RA-induced increase of *PBX1* levels, decreased proliferation and induced RA-independent differentiation in those cell lines. SK-N-SH cells differentiate with a markedly different phenotype compared to SHSY5Y and SK-N-BE(2) cells when exposed to 13-*cisRA*, although all are N-type cell lines(Figure 4, Supplementary Figure 2). SK-N-SH cells differentiate into spindle-shaped cells that express neuronal proteins, in marked contrast to the subcloned cell line SHSY5Y.

SHSY5Y and SK-N-BE(2) cells differentiate into neuronal cells with narrow neurites, typical of other N-type cells. SK-N-BE(2) cells are MYCN-amplified, in contrast to the other cell lines used. PBX1 induced differentiation similar to that induced by 13-*cis*RA in each cell line, suggesting PBX1 acts through a common mechanism in NB even with different biology.

We observed in SK-N-RA cells that increased PBX1 expression caused significant increases in TUBB3 expression, decreased proliferation, and increased RA sensitivity, though less profoundly as in the other cell lines. We further observed no significant change in NTRK1 expression in SK-N-RA due to PBX1, which may prevent differentiation (Figure 3D). Thus, PBX1 may be necessary but not sufficient for terminal differentiation in NB. A similar role for PBX1 in terminal differentiation has been observed in adipocytes(42) and osteoblasts(43). Investigations into how PBX1 functions in normal neuroblasts and neuroblastoma will elucidate the differentiation process in NB, and how differentiation is avoided in RA-resistant NB.

NB cells express two PBX1 isoforms, PBX1a and PBX1b. The longer PBX1a isoform was expressed more strongly qualitatively in most RA-sensitive cell lines, and increased with 13-*cis* RA, but not the RA-resistant cell lines. Differential functions of PBX isoforms are found in normal biology(44) and cancers(45, 46). PBX1b acts as a transcriptional activator through recruitment of chromatin remodeling proteins(47) including CBP, a histone acetyltransferase (HAT)(44). PBX1b may act to maintain an undifferentiated phenotype in normal neuroblasts and neuroblastoma, as it is generally expressed in embryonic tissues(45). PBX1a, in contrast, acts as a transcriptional repressor through recruitment of complexes including NCOR2 and HDACs(44). Increased differential PBX1a expression may drive differentiation, consistent with its expression in mature tissues(45). Studies into PBX1 isoform functions and the regulation of differential *PBX1* splicing will be important in understanding their roles in neuroblast development. PBX1 paralogs PBX2-4 share homology and can also be induced by retinoids in other tissues(15), so studies into their functions will further define their effects on NB differentiation. For example, these paralogs could functionally replace or competitively inhibit PBX1 in NB differentiation.

Our findings suggest PBX1 acts to inhibit proliferation in NB and may induce spontaneous differentiation in patients with low-risk disease. This is substantiated by the significantly higher *PBX1* expression levels in benign ganglioneuromas and low-risk NB samples cured surgically, compared to low-risk and intermediate-risk tumors needing chemotherapy for definitive cure. Subgroup analysis of the Khan dataset similarly demonstrated significantly lower *PBX1* expression in patients <18 months of age with recurrent disease compared to those cured surgically. In both sample sets, there is 30-fold difference in median expression between recurrent low-risk tumors and nonrecurrent tumors with no overlap in the range of expression between groups.

The INRG Risk Classification system defines “very-low” and “low-risk” patients expected to have >75% 5-year EFS after surgery alone(5). No biomarkers identify patients within those groups who do not need tumor resection for disease control, or those patients who will need adjuvant treatment. Our research indicates *PBX1* may serve as such a biomarker in

low-risk NB, despite the small sample number, particularly given the large difference in *PBX1* expression. A larger study of *PBX1* expression in low-risk disease is warranted to validate the threshold of stratification and correlate mRNA expression with protein expression measured by immunohistochemistry (IHC). Ideally, after vigorous validation of our findings, *PBX1* expression would be used as a biomarker of differentiation in patients risk-stratified as “low” or “very-low” risk by INRG criteria. Those patients’ tumors would be tested for *PBX1* expression, by RT-qPCR or IHC. Those with “high” expression would be managed with observation without surgery, and those with “low” expression would be recommended for surgery and adjuvant chemotherapy.

It is noteworthy that, unlike in NB cell lines, “basal” *PBX1* tumor expression correlates with tumor grade and treatment outcome. This may be due to the origination of most NB cell lines, including all used in this study, from patients with Stage 4 disease. Tumors from those patients would be expected to have low *PBX1* expression, consistent with our analyses of primary human tumors. Furthermore, NB inherently has perturbations in differentiation; we found that the degree of differentiation correlated with *PBX1* expression in cell lines and tumors (i.e., the more *PBX1* observed, the more differentiated the cells). Accordingly, it is not surprising that low-risk surgically-cured NB and terminally-differentiated ganglioneuromas have significantly higher *PBX1* expression than more aggressive disease; differentiated tumors have responded to endogenous factors normally expressed in children, and more aggressive tumors have not. The lack of differential *PBX1* expression in the subsets of high-risk disease may reflect the heterogeneity of the cohort, as they ranged from Stage 2–4 and nonsurvivors progressed at various points in therapy. Alternately, *PBX1* may exert its effects in tumor cells at a more differentiated state than in high-risk disease, or in an isoform-specific manner, further emphasizing our future studies into *PBX1* isoforms. A pilot study examining only patients with recurrent disease, after receiving 13-*cisRA*, may clarify if *PBX1* is most important in terminal differentiation.

Evaluation of *PBX1* expression in three clinical NB cohorts demonstrated its potential utility as a biomarker in high-risk disease. *PBX1* is particularly powerful prognostically in the Seeger dataset of metastatic *MYCN*-nonamplified NB, the subgroup of patients that would most benefit from a validated biomarker. *PBX1* expression also was independently prognostic in multivariate analysis in the larger heterogeneous Oberthuer cohort including *MYCN*-amplified and nonamplified patients. It was more significant than age, stage, and *MYCN* amplification, well-established biomarkers of aggressive disease even in patients with localized tumors(5). Although multivariate analysis was limited in the Khan dataset due to small sample size and homogenous patient characteristics, *PBX1* expression was prognostic of survival even in this cohort. The significant survival difference appreciated in these sets based on *PBX1* expression and including high-risk patients, may be explained by the microarrays used. The probes used hybridize to the 3’ end of *PBX1*, where the differences in the isoforms are, and the analysis may have unveiled an isoform-specific difference (e.g., the arrays identify *PBX1a* specifically). Future studies could reasonably evaluate if *PBX1* expression distinguishes high-risk patients for whom current therapies are ineffective from those who benefit from standard therapy, in a similar approach to that described for low-risk disease. It may be particularly useful for high-risk *MYCN*-

nonamplified disease. Despite INRG Risk Classification criteria(48), there are no validated predictors of therapeutic resistance for these patients and recently identified biomarkers have proven ineffective(49).

Our work has identified low PBX1 expression as a novel biomarker of disease aggression in NB, and laboratory findings define a role for PBX1 in NB differentiation. This biomarker may serve to better define risk for patients with both low-risk disease and MYCN-nonamplified high-risk disease through future prospective trials. These data anticipate a therapeutic potential for patients by modulating the pathways that affect PBX1 expression.

Supplementary Material

Refer to Web version on PubMed Central for supplementary material.

Acknowledgments

Financial Support: Conquer Cancer Foundation Young Investigator Award and NCH Internal Fund 187213 to NS; Burroughs Wellcome Clinical Scientist in Translational Research and NIH grants R01CA133662, R01CA138212, and RC4CA156509 for JT.

References

1. Park JR, Eggert A, Caron H. Neuroblastoma: biology, prognosis, and treatment. *Pediatr Clin North Am.* 2008; 55:97–120. x. [PubMed: 18242317]
2. Hero B, Simon T, Spitz R, Ernestus K, Gnekow AK, Scheel-Walter HG, et al. Localized infant neuroblastomas often show spontaneous regression: results of the prospective trials NB95-S and NB97. *J Clin Oncol.* 2008; 26:1504–10. [PubMed: 18349403]
3. Yu AL, Gilman AL, Ozkaynak MF, London WB, Kreissman SG, Chen HX, et al. Anti-GD2 antibody with GM-CSF, interleukin-2, and isotretinoin for neuroblastoma. *N Engl J Med.* 2010; 363:1324–34. [PubMed: 20879881]
4. Matthay KK, Villablanca JG, Seeger RC, Stram DO, Harris RE, Ramsay NK, et al. Children's Cancer Group. Treatment of high-risk neuroblastoma with intensive chemotherapy, radiotherapy, autologous bone marrow transplantation, and 13-cis-retinoic acid. *N Engl J Med.* 1999; 341:1165–73. [PubMed: 10519894]
5. Cohn SL, Pearson AD, London WB, Monclair T, Ambros PF, Brodeur GM, et al. The International Neuroblastoma Risk Group (INRG) classification system: an INRG Task Force report. *J Clin Oncol.* 2009; 27:289–97. [PubMed: 19047291]
6. Brodeur GM, Seeger RC, Schwab M, Varmus HE, Bishop JM. Amplification of N-myc in untreated human neuroblastomas correlates with advanced disease stage. *Science.* 1984; 224:1121–4. [PubMed: 6719137]
7. Schleiermacher G, Michon J, Ribeiro A, Pierron G, Mosseri V, Rubie H, et al. Segmental chromosomal alterations lead to a higher risk of relapse in infants with MYCN-non-amplified localised unresectable/disseminated neuroblastoma (a SIOPEN collaborative study). *Br J Cancer.* 2011; 105:1940–8. [PubMed: 22146831]
8. Spitz R, Hero B, Ernestus K, Berthold F. Deletions in chromosome arms 3p and 11q are new prognostic markers in localized and 4s neuroblastoma. *Clinical cancer research: an official journal of the American Association for Cancer Research.* 2003; 9:52–8. [PubMed: 12538451]
9. Lau DT, Hesson LB, Norris MD, Marshall GM, Haber M, Ashton LJ. Prognostic significance of promoter DNA methylation in patients with childhood neuroblastoma. *Clin Cancer Res.* 2012; 18:5690–700. [PubMed: 22929802]
10. Mohlin SA, Wigerup C, Pahlman S. Neuroblastoma aggressiveness in relation to sympathetic neuronal differentiation stage. *Semin Cancer Biol.* 2011; 21:276–82. [PubMed: 21945591]

11. Manohar CF, Salwen HR, Furtado MR, Cohn SL. Up-regulation of HOXC6, HOXD1, and HOXD8 homeobox gene expression in human neuroblastoma cells following chemical induction of differentiation. *Tumour Biol.* 1996; 17:34–47. [PubMed: 7501971]
12. Mao L, Ding J, Zha Y, Yang L, McCarthy BA, King W, et al. HOXC9 links cell-cycle exit and neuronal differentiation and is a prognostic marker in neuroblastoma. *Cancer research.* 2011; 71:4314–24. [PubMed: 21507931]
13. Brendolan A, Ferretti E, Salsi V, Moses K, Quaggin S, Blasi F, et al. A Pbx1-dependent genetic and transcriptional network regulates spleen ontogeny. *Development.* 2005; 132:3113–26. [PubMed: 15944191]
14. Qin P, Haberbusch JM, Zhang Z, Soprano KJ, Soprano DR. Pre-B cell leukemia transcription factor (PBX) proteins are important mediators for retinoic acid-dependent endodermal and neuronal differentiation of mouse embryonal carcinoma P19 cells. *J Biol Chem.* 2004; 279:16263–71. [PubMed: 14742427]
15. Knoepfler PS, Kamps MP. The Pbx family of proteins is strongly upregulated by a post-transcriptional mechanism during retinoic acid-induced differentiation of P19 embryonal carcinoma cells. *Mech Dev.* 1997; 63:5–14. [PubMed: 9178252]
16. Vitobello A, Ferretti E, Lampe X, Vilain N, Ducret S, Ori M, et al. Hox and Pbx factors control retinoic acid synthesis during hindbrain segmentation. *Dev Cell.* 2011; 20:469–82. [PubMed: 21497760]
17. Kim SK, Selleri L, Lee JS, Zhang AY, Gu X, Jacobs Y, et al. Pbx1 inactivation disrupts pancreas development and in *Ipfl*-deficient mice promotes diabetes mellitus. *Nat Genet.* 2002; 30:430–5. [PubMed: 11912494]
18. Chen JL, Li J, Kiriluk KJ, Rosen AM, Paner GP, Antic T, et al. Deregulation of a Hox protein regulatory network spanning prostate cancer initiation and progression. *Clin Cancer Res.* 2012; 18:4291–302. [PubMed: 22723371]
19. Magnani L, Ballantyne EB, Zhang X, Lupien M. PBX1 genomic pioneer function drives ERalpha signaling underlying progression in breast cancer. *PLoS Genet.* 2011; 7:e1002368. [PubMed: 22125492]
20. Shiraishi K, Yamasaki K, Nanba D, Inoue H, Hanakawa Y, Shirakata Y, et al. Pre-B-cell leukemia transcription factor 1 is a major target of promyelocytic leukemia zinc-finger-mediated melanoma cell growth suppression. *Oncogene.* 2007; 26:339–48. [PubMed: 16862184]
21. Kamps MP, Murre C, Sun XH, Baltimore D. A new homeobox gene contributes the DNA binding domain of the t(1;19) translocation protein in pre-B ALL. *Cell.* 1990; 60:547–55. [PubMed: 1967983]
22. Foley J, Cohn SL, Salwen HR, Chagnovich D, Cowan J, Mason KL, et al. Differential expression of N-myc in phenotypically distinct subclones of a human neuroblastoma cell line. *Cancer Res.* 1991; 51:6338–45. [PubMed: 1933896]
23. Biedler JL, Helson L, Spengler BA. Morphology and growth, tumorigenicity, and cytogenetics of human neuroblastoma cells in continuous culture. *Cancer Res.* 1973; 33:2643–52. [PubMed: 4748425]
24. Keshelava N, Seeger RC, Groshen S, Reynolds CP. Drug resistance patterns of human neuroblastoma cell lines derived from patients at different phases of therapy. *Cancer Res.* 1998; 58:5396–405. [PubMed: 9850071]
25. Reynolds CP, Biedler JL, Spengler BA, Reynolds DA, Ross RA, Frenkel EP, et al. Characterization of human neuroblastoma cell lines established before and after therapy. *J Natl Cancer Inst.* 1986; 76:375–87. [PubMed: 3456456]
26. Biedler JL, Roffler-Tarlov S, Schachner M, Freedman LS. Multiple neurotransmitter synthesis by human neuroblastoma cell lines and clones. *Cancer Res.* 1978; 38:3751–7. [PubMed: 29704]
27. Tumilowicz JJ, Nichols WW, Cholon JJ, Greene AE. Definition of a continuous human cell line derived from neuroblastoma. *Cancer Res.* 1970; 30:2110–8. [PubMed: 5459762]
28. Seeger RC, Rayner SA, Banerjee A, Chung H, Laug WE, Neustein HB, et al. Morphology, growth, chromosomal pattern and fibrinolytic activity of two new human neuroblastoma cell lines. *Cancer Res.* 1977; 37:1364–71. [PubMed: 856461]

29. Tsokos M, Scarpa S, Ross RA, Triche TJ. Differentiation of human neuroblastoma recapitulates neural crest development. Study of morphology, neurotransmitter enzymes, and extracellular matrix proteins. *The American journal of pathology*. 1987; 128:484–96. [PubMed: 2888312]
30. Oberthuer A, Berthold F, Warnat P, Hero B, Kahlert Y, Spitz R, et al. Customized oligonucleotide microarray gene expression-based classification of neuroblastoma patients outperforms current clinical risk stratification. *Journal of clinical oncology: official journal of the American Society of Clinical Oncology*. 2006; 24:5070–8. [PubMed: 17075126]
31. Wei JS, Greer BT, Westermann F, Steinberg SM, Son CG, Chen QR, et al. Prediction of clinical outcome using gene expression profiling and artificial neural networks for patients with neuroblastoma. *Cancer research*. 2004; 64:6883–91. [PubMed: 15466177]
32. Asgharzadeh S, Pique-Regi R, Sposto R, Wang H, Yang Y, Shimada H, et al. Prognostic significance of gene expression profiles of metastatic neuroblastomas lacking MYCN gene amplification. *J Natl Cancer Inst*. 2006; 98:1193–203. [PubMed: 16954472]
33. Thiele CJ, Reynolds CP, Israel MA. Decreased expression of N-myc precedes retinoic acid-induced morphological differentiation of human neuroblastoma. *Nature*. 1985; 313:404–6. [PubMed: 3855502]
34. Reynolds CP, Wang Y, Melton LJ, Einhorn PA, Slamon DJ, Maurer BJ. Retinoic-acid-resistant neuroblastoma cell lines show altered MYC regulation and high sensitivity to fenretinide. *Med Pediatr Oncol*. 2000; 35:597–602. [PubMed: 11107126]
35. Lucarelli E, Kaplan DR, Thiele CJ. Selective regulation of TrkA and TrkB receptors by retinoic acid and interferon-gamma in human neuroblastoma cell lines. *J Biol Chem*. 1995; 270:24725–31. [PubMed: 7559588]
36. Light JE, Koyama H, Minturn JE, Ho R, Simpson AM, Iyer R, et al. Clinical significance of NTRK family gene expression in neuroblastomas. *Pediatr Blood Cancer*. 2011; 59:226–32. [PubMed: 21990266]
37. Wang LL, Suganuma R, Ikegaki N, Tang X, Naranjo A, McGrady P, et al. Neuroblastoma of undifferentiated subtype, prognostic significance of prominent nucleolar formation, and MYC/MYCN protein expression: a report from the Children’s Oncology Group. *Cancer*. 2013; 119:3718–26. [PubMed: 23901000]
38. Tischfield MA, Baris HN, Wu C, Rudolph G, Van Maldergem L, He W, et al. Human TUBB3 mutations perturb microtubule dynamics, kinesin interactions, and axon guidance. *Cell*. 2010; 140:74–87. [PubMed: 20074521]
39. Brodeur GM, Seeger RC, Barrett A, Berthold F, Castleberry RP, D’Angio G, et al. International criteria for diagnosis, staging, and response to treatment in patients with neuroblastoma. *J Clin Oncol*. 1988; 6:1874–81. [PubMed: 3199170]
40. Giannini G, Di Marcotullio L, Ristori E, Zani M, Crescenzi M, Scarpa S, et al. HMGI(Y) and HMGI-C genes are expressed in neuroblastoma cell lines and tumors and affect retinoic acid responsiveness. *Cancer research*. 1999; 59:2484–92. [PubMed: 10344762]
41. Holzel M, Huang S, Koster J, Ora I, Lakeman A, Caron H, et al. NF1 is a tumor suppressor in neuroblastoma that determines retinoic acid response and disease outcome. *Cell*. 2010; 142:218–29. [PubMed: 20655465]
42. Monteiro MC, Sanyal M, Cleary ML, Sengenes C, Bouloumie A, Dani C, et al. PBX1: a novel stage-specific regulator of adipocyte development. *Stem Cells*. 2011; 29:1837–48. [PubMed: 21922607]
43. Gordon JA, Hassan MQ, Saini S, Montecino M, van Wijnen AJ, Stein GS, et al. Pbx1 represses osteoblastogenesis by blocking Hoxa10-mediated recruitment of chromatin remodeling factors. *Mol Cell Biol*. 2010; 30:3531–41. [PubMed: 20439491]
44. Asahara H, Dutta S, Kao HY, Evans RM, Montminy M. Pbx-Hox heterodimers recruit coactivator-corepressor complexes in an isoform-specific manner. *Mol Cell Biol*. 1999; 19:8219–25. [PubMed: 10567547]
45. Schnabel CA, Selleri L, Jacobs Y, Warnke R, Cleary ML. Expression of Pbx1b during mammalian organogenesis. *Mech Dev*. 2001; 100:131–5. [PubMed: 11118899]
46. Crijns AP, de Graeff P, Geerts D, Ten Hoor KA, Hollema H, van der Sluis T, et al. MEIS and PBX homeobox proteins in ovarian cancer. *Eur J Cancer*. 2007; 43:2495–505. [PubMed: 17949970]

47. Berkes CA, Bergstrom DA, Penn BH, Seaver KJ, Knoepfler PS, Tapscott SJ. Pbx marks genes for activation by MyoD indicating a role for a homeodomain protein in establishing myogenic potential. *Mol Cell*. 2004; 14:465–77. [PubMed: 15149596]
48. Spitz R, Hero B, Simon T, Berthold F. Loss in chromosome 11q identifies tumors with increased risk for metastatic relapses in localized and 4S neuroblastoma. *Clinical cancer research: an official journal of the American Association for Cancer Research*. 2006; 12:3368–73. [PubMed: 16740759]
49. Oberthuer A, Warnat P, Kahlert Y, Westermann F, Spitz R, Brors B, et al. Classification of neuroblastoma patients by published gene-expression markers reveals a low sensitivity for unfavorable courses of MYCN non-amplified disease. *Cancer letters*. 2007; 250:250–67. [PubMed: 17126996]
50. Reynolds CP, Matthay KK, Villablanca JG, Maurer BJ. Retinoid therapy of high-risk neuroblastoma. *Cancer letters*. 2003; 197:185–92. [PubMed: 12880980]
51. de The H, Vivanco-Ruiz MM, Tiollais P, Stunnenberg H, Dejean A. Identification of a retinoic acid responsive element in the retinoic acid receptor beta gene. *Nature*. 1990; 343:177–80. [PubMed: 2153268]
52. Wang J, Yen A. A novel retinoic acid-responsive element regulates retinoic acid-induced BLR1 expression. *Mol Cell Biol*. 2004; 24:2423–43. [PubMed: 14993281]
53. Martin PJ, Delmotte MH, Formstecher P, Lefebvre P. PLZF is a negative regulator of retinoic acid receptor transcriptional activity. *Nuclear receptor*. 2003; 1:6. [PubMed: 14521715]
54. Chen Z, Guidez F, Rousselot P, Agadir A, Chen SJ, Wang ZY, et al. PLZF-RAR alpha fusion proteins generated from the variant t(11;17)(q23;q21) translocation in acute promyelocytic leukemia inhibit ligand-dependent transactivation of wild-type retinoic acid receptors. *Proceedings of the National Academy of Sciences of the United States of America*. 1994; 91:1178–82. [PubMed: 8302850]
55. Kikugawa T, Kinugasa Y, Shiraishi K, Nanba D, Nakashiro K, Tanji N, et al. PLZF regulates Pbx1 transcription and Pbx1-HoxC8 complex leads to androgen-independent prostate cancer proliferation. *The Prostate*. 2006; 66:1092–9. [PubMed: 16637071]

Translational Relevance

NB arises from neural crest progenitor cells, but the errors in differentiation that drive tumorigenesis remain cryptic. We identify *PBX1* as a putative critical regulator of differentiation in NB. Clinically, NB presents diversely in children. The majority of tumors in infants undergo spontaneous involution or differentiation, but some patients require chemotherapy to be cured. Most patients greater than 18 months old, in contrast, present with high-risk metastatic disease. Some patients benefit from multimodal treatment including 13-*cis*RA, but there are no clinically validated biomarkers that predict benefit for high-risk patients. Patient tumors with low *PBX1* expression may indicate more aggressive disease in both low-risk and high-risk NB. Our work supports validation of *PBX1* expression as a risk factor for treatment stratification in patients with low-risk and high-risk NB, and also supports further studies into the regulation of *PBX1* and targeted therapeutics for treatment-resistant disease.

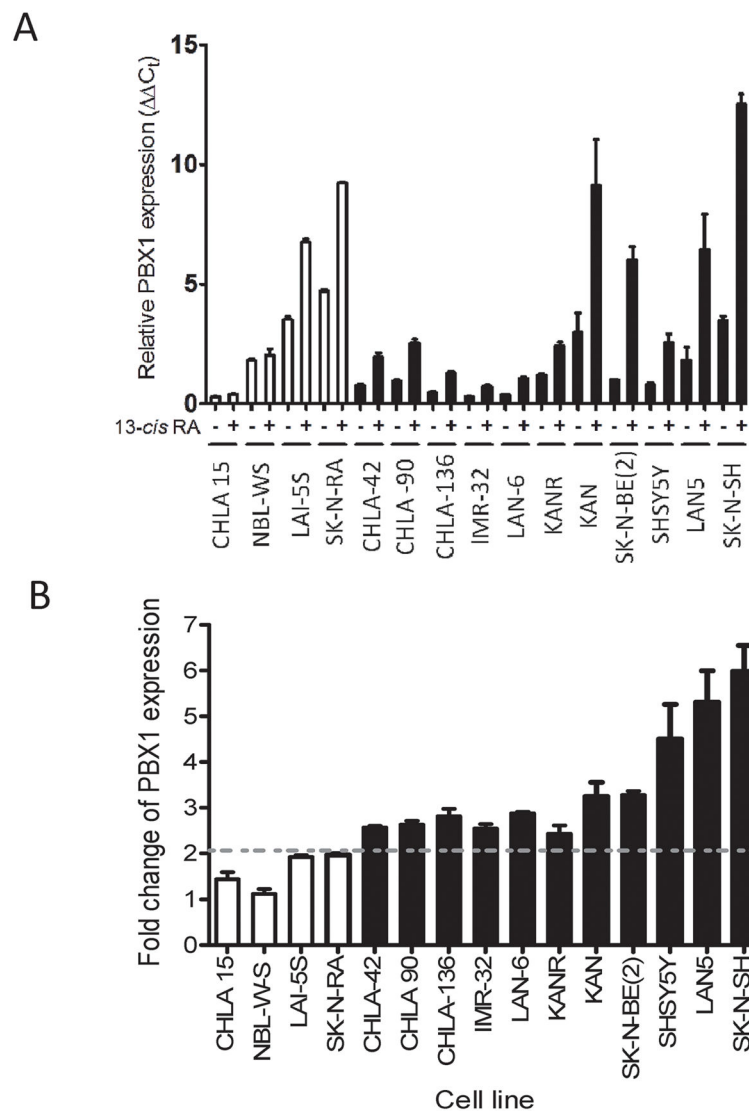


Figure 1. *PBX1* is specifically upregulated in RA-sensitive NB cell lines in the presence of 13-*cisRA*

A) Expression of *PBX1* mRNA, as analyzed by RT-qPCR, in 4 RA-resistant NB cell lines (white) and 11 RA sensitive NB cell lines (black). B) Fold-change in expression of *PBX1* mRNA in the presence of 13-*cisRA*. RA-sensitive vs resistant lines compared by Student's t-test.

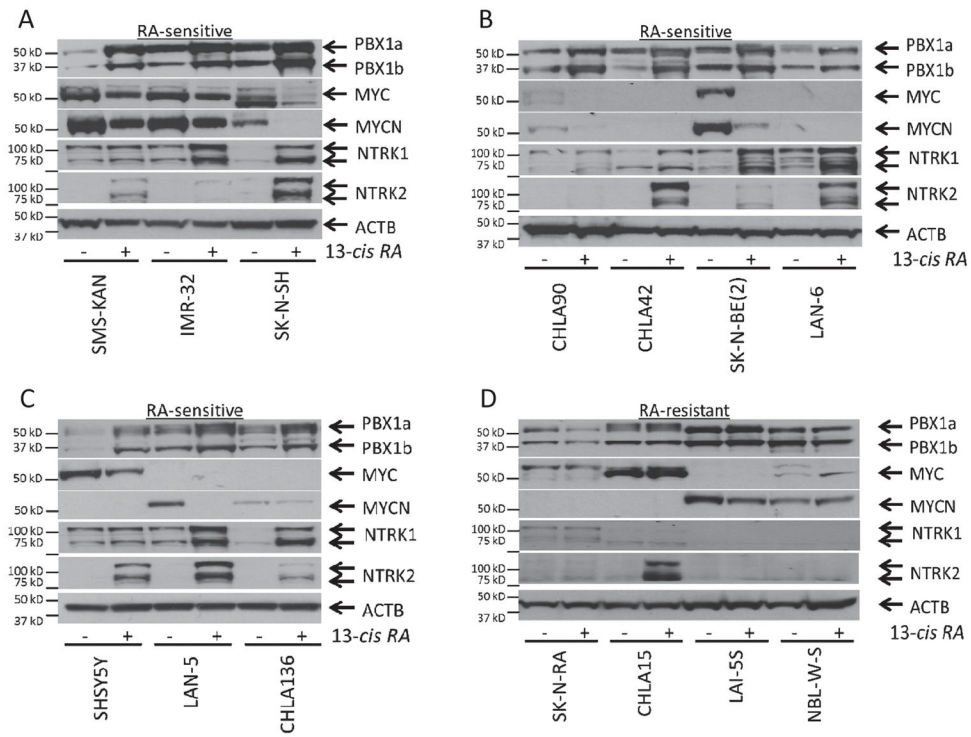


Figure 2. PBX1 is upregulated in RA-sensitive NB cell lines and correlates with markers of response to 13-cisRA

Western blot analysis of PBX1, MYC, MYCN, NTRK1, AND NTRK2 expression in 14 NB cell lines. A–C) Western blots of RA-sensitive cell lines. D) Western blots of RA-resistant cell lines. Full uncut Western Blots, including controls, available in supplementary data.

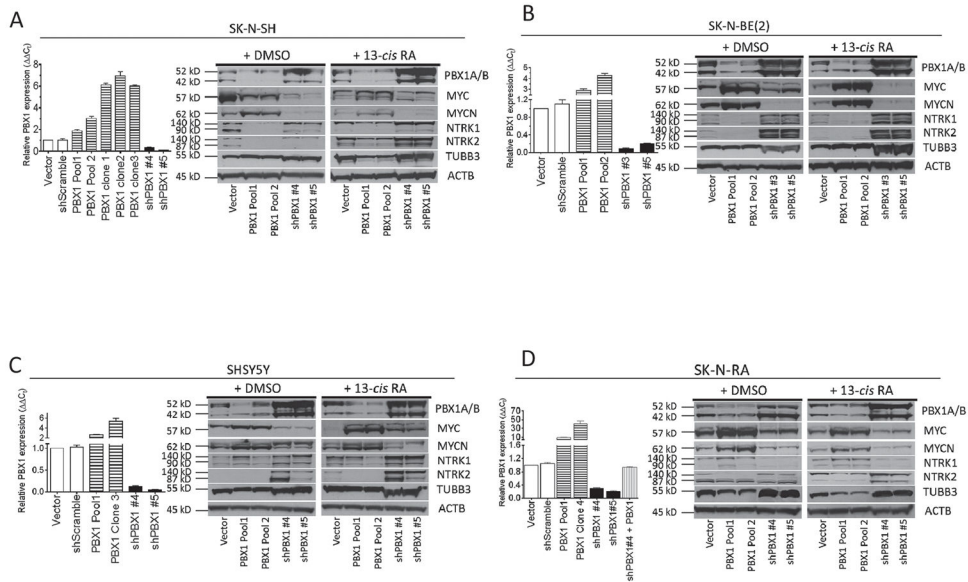


Figure 3. PBX1 level correlates with markers of neuronal differentiation

Modulation of PBX1 expression in four NB cell lines. Using RA-sensitive cell lines SK-N-SH (A), SK-N-BE(2) (B), SHSY5Y (C) and RA-resistant NB cell line SK-N-RA (D), *PBX1* was exogenously expressed by plasmid transfection or reduced using shRNA constructs. Relative expression was measured by RT-qPCR (bar graphs), standardized to expression of *18S RNA*. PBX1 expression in each cell population was compared to vector control for each cell line type. Western blot analysis of expression of isoforms PBX1a and PBX1b, MYC, MYCN, NTRK1, NTRK2, TUBB2, and ACTB in stably derived NB cells described in (A–D) cultured in 0.1% DMSO or 10 μ M 13-*cis*RA for 5 days. Full uncut Western blots including controls available in supplementary data.

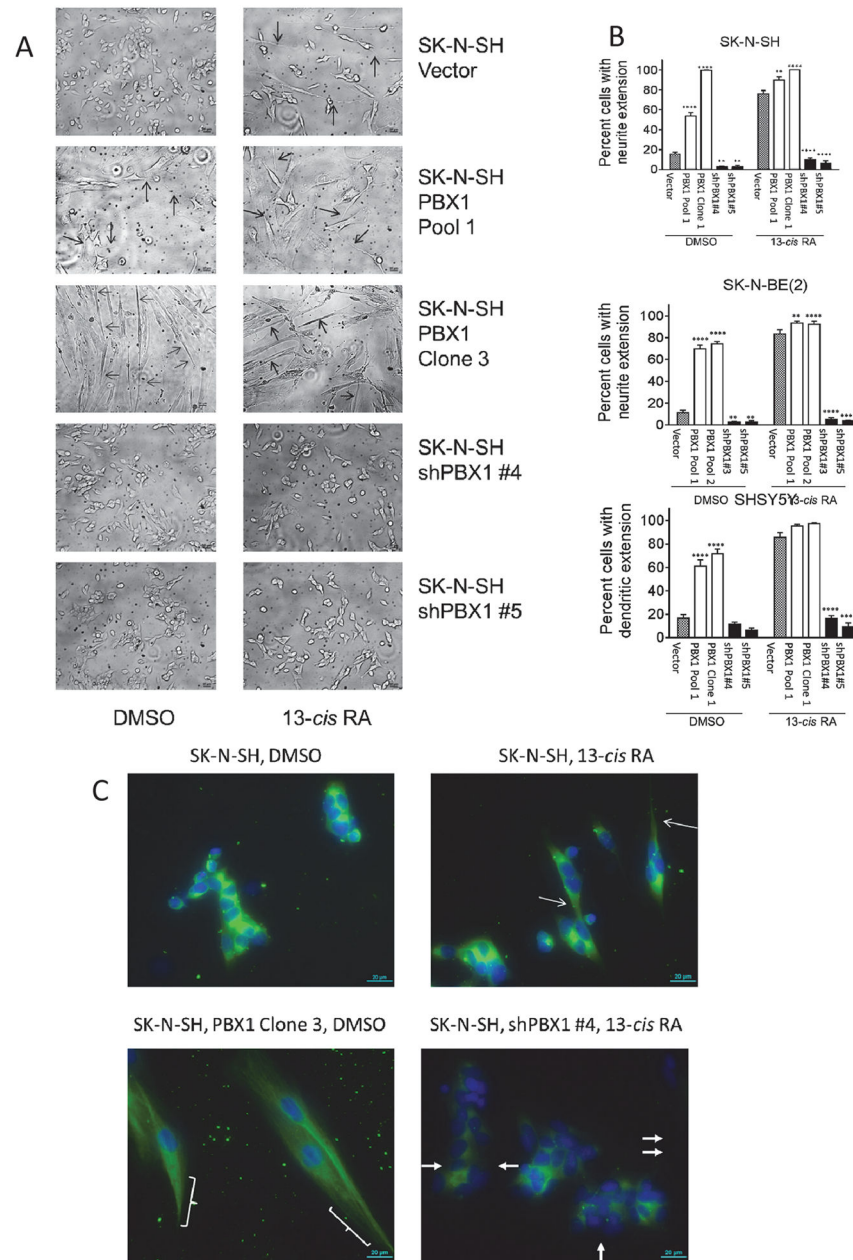


Figure 4. Morphologic changes in SK-N-SH cells correlate with PBX1 expression

A) Cells were grown in complete media with either DMSO or 10 μ M 13-*cis*RA for 7 days, then observed under 10X magnification. Neurite extensions are indicated with open arrows. B–D) Percentage of cells (SK-N-SH, figure B; SK-N-BE(2), figure C; SHSY5Y, figure D) with neurite extension, defined as cells with at least one neurite > the length of the cell body. 100 cells of each type were counted and the percent of cells with neurite extension noted; this was performed in triplicate and compared to vector control by Student's t-test, **: $p < 0.01$; ****: $p < 0.0001$. D) Immunofluorescence of TUBB3 in SK-N-SH cells. Complete sets of images can be found in the Supplementary Data. Thin arrows and brackets indicate

neurite extensions. Filled arrows indicate cells without TUBB3 expression. Green =TUBB3; blue = nucleus. Total PBX1 and TUBB3 expression is measured in Figure 2.

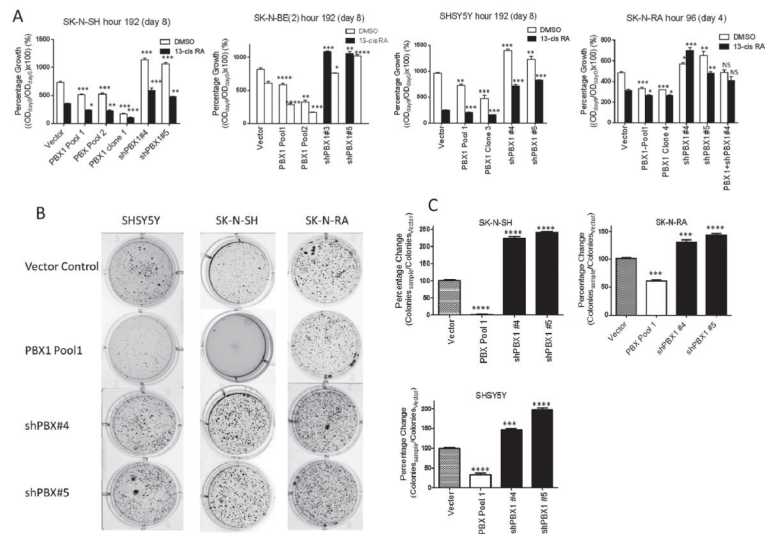


Figure 5. PBX1 expression inversely correlates with cell proliferation, directly with responsiveness to 13-cisRA, and inversely with anchorage-independent tumor sphere formation

A) Percentage growth of each cell line in DMSO control (white bars) or 13-cisRA (black bars), as compared to cell count at time 0. Significant difference of each cell line versus vector control under same growth condition is marked, compared by Student's t-test. PBX1 protein levels are shown in Figure 2. *: $p < 0.05$, **: $p < 0.01$, ***: $p < 0.001$ ****: $p < 0.0001$. B) Photographs of tumor spheres grown in soft agar. Cells were plated at density of 5000 cells/well, in triplicate, in 0.3% low melting point agarose/RPMI complete and allowed to grow for 1 month. Cells were then stained with MTT and colonies counted. Representative wells are shown. C) Quantitation of colonies. Colonies were counted and compared to control cells and entered as a percentage, and compared by Student's t-test, ***: $p < 0.001$. ****: $p < 0.0001$. PBX1 protein levels shown in Figure 2.

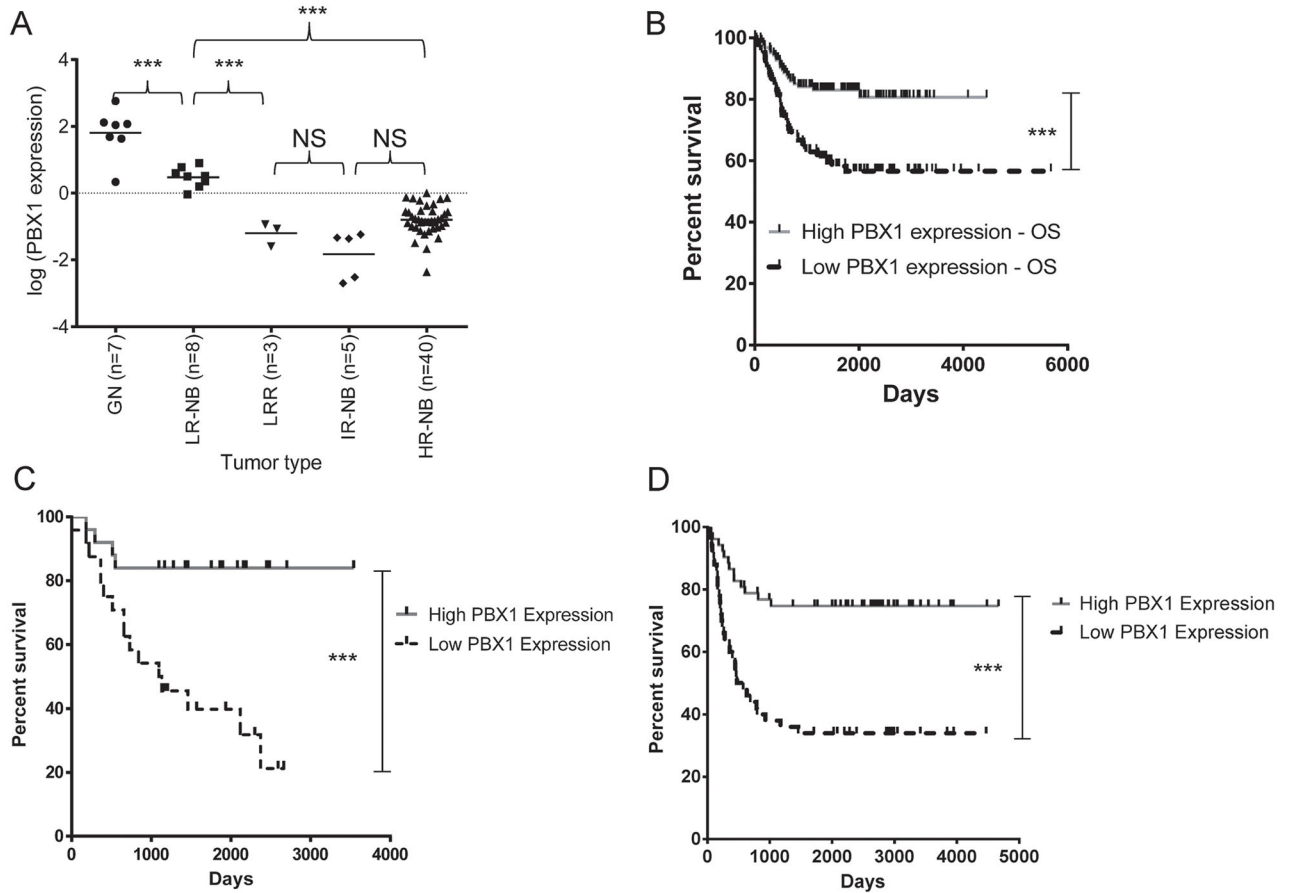


Figure 6. *PBX1* expression correlates with tumor histology and risk, and is prognostic for survival

A) *PBX1* expression in benign ganglioneuromas (GN), low-risk NB cured surgically (LR-NB), recurrent low-risk NB (LRR), intermediate-risk NB cured with chemotherapy (IR-NB), and high-risk NB (HR-NB). Relative *PBX1* expression was measured by RT-qPCR and calculated using the 2^{-C_t} method, using *PBX1* expression in SHSY5Y cells as a baseline comparison. Significant differences noted between groups were calculated by one-way ANOVA. B) Overall univariate survival comparison using *PBX1* expression of the Oberthuer dataset of 251 patients of all stages ($p=0.0004$). Median expression of *PBX1* was used to stratify patients high (grey solid) versus low (black dashed) *PBX1* expression in this graph and all other survival curves. C) OS analysis of the Khan dataset of 49 patients of all stages ($p=0.00125$). D) OS analysis of the Seeger dataset of 102 patients with metastatic, MYCN-nonamplified NB ($p=0.0002$).